JOURNAL OF GEOPHYSICAL RESEARCH, VOL. 106, NO. E3, PAGES 5107–5121, MARCH 25, 2001

Thermal convection in the outer shell of large icy satellites

Frédéric Deschamps[1] and Christophe Sotin
Laboratoire de Planétologie et Géodynamique, UMR-CNRS 6112, Université de Nantes, Nantes, France

Abstract. Evolution of large icy satellites is controlled by heat transfer across the outer ice I layer. After the core overturn a possible structure consists of a silicate core and a shell of molten ices. As the satellite cools down, the primordial ocean crystallizes. If the outer layer is thick enough, convection is very likely to occur in it. We have used the results of a recent two-dimensional numerical model of convection including variable viscosity to estimate the vigor and the efficiency of convection in this layer. Viscosity variations induce the apparition of a stagnant lid at the top of the fluid, which reduces the efficiency of heat transfer. In the present study, the Rayleigh number *Ra* and the heat flux Φ are computed as a function of the thickness of the layer, assuming that the ice flow is Newtonian. Calculations are first made for a generic satellite of radius $R = 2500$ km and mean density $\langle\rho\rangle = 1.9$ g/cm^3. It is then shown that variations of ±500 km on the radius and ±0.5 g/cm^3 on the mean density do not induce significant differences in the values of *Ra* and Φ. On the other hand, variations of the reference viscosity μ_0, and of the activation energy E induce major differences. The reference viscosity is equal to the viscosity close to the melting point, and its possible value yields around $\mu_0 = 5\times10^{13}$ Pa s. A possible value of E is 60 kJ/mol. For these values of the rheological parameters we find that the initial ocean may crystallize completely in ~3.6 Gyr. Higher values of μ_0 and/or E reduce significantly the vigor and the efficiency of convection. The influence of the composition of the initial ocean is also investigated. The presence of ammonia reduces the convective strength and the heat flux. The upper structure of icy satellites is discussed as a function of the rheological and compositional parameters. The presence of a sub-surface ocean could be explained by either the presence of volatiles in the initial ocean or the presence of additional heat sources, such as tidal dissipation.

1. Introduction

Results from the Galileo mission have increased the scientific interest in knowledge of the internal structure of large icy satellites. An important question is the possible existence of a subsurface ocean, as it has been suggested in the case of Europa [*Carr et al.*, 1998; *Kivelson et al.*, 2000]. The measurements of the dimensionless polar moment of inertia (J), recently performed by Galileo, has put important constraints on the internal structure of Jupiter's main satellites. For Ganymede the value of J is small (see Table 1), indicating that its possible structure consists of a metallic core, a silicate mantle, and an ice/water outer shell [*Anderson et al.*, 1996]. Europa might also have differentiated in a metallic core [*Anderson et al.*, 1998b]. Because of the lack of tectonic features at its surface, Callisto was first understood as an undifferentiated body [*Schubert et al.*, 1981; *Friedson and Stevenson*, 1983]. However, the measurements provided by Galileo indicated that Callisto is, in fact, slightly differentiated [*Anderson et al.*, 1998a] (Table 1). Moreover, magnetic perturbations recorded near Callisto could be explained by the presence of a subsurface ocean [*Khurana et al.*, 1998; *Zimmer et al.*, 2000].

The value of J alone does not allow the determination of an accurate structure. To compute such a structure, evolutionary models must be elaborated. *Lewis* [1971] demonstrated that the early thermal evolution of large icy satellites could induce a differentiated structure. Indeed, many authors have proposed differentiated structures for the large satellites of Jupiter [e.g., *Consolmagno and Lewis*, 1976; *Reynolds and Cassen*, 1979; *Cassen et al.*, 1981; *Schubert et al.*, 1981]. They showed that such models could explain the mean densities of these bodies as well as the observations reported by the Voyager probes. Differentiated models have also been proposed for Titan, the largest satellite of Saturn [*Kirk and Stevenson, 1987*; *Grasset and Sotin*, 1996]. Titan is similar to Ganymede in size and density, but its surface is hidden by a thick atmosphere. In these models an icy shell is formed by the crystallization of a primordial ocean as the satellite cools down. As it is growing, the outer shell becomes unstable and starts to convect. The ocean is assumed to be perfectly adiabatic, and therefore the outer ice shell may control the cooling of the satellite and the evolution of its upper structure. For instance, if heat transfer is not efficient enough, the crystallization of the ocean cannot be completed. Two possible scenarios are sketched in Figure 1.

To estimate the convective heat flux, one usually uses a scaling law relating the Nusselt number *Nu*, which measures the efficiency of convection, to the Rayleigh number *Ra*, which measures the strength of convection. Previous studies have used scaling laws that do not account for viscosity variations. However, the viscosity of ice I is strongly temperature-dependent [e.g., *Goodman et al.*, 1981; *Weertman*, 1983], and it is well established that the vigor and the efficiency of convection, as well as the flow pattern, are very sensitive to viscosity variations [*Nataf and Richter*, 1982; *White*, 1988; *Ogawa et al.*, 1991]. Previous studies accounted for viscosity variations of ice I with

[1] Now at Faculty of Earth Sciences, Utrecht University, Utrecht, Netherlands.

Paper number 2000JE001253
0148-0227/01/2000JE001253$09.00

Table 1. Physical Properties of Large Icy Satellites

Satellite	Diameter		g	Mass		$\langle\rho\rangle$	$J=C/Ma^2$
	km	Moon=1	m/s^2	10^{23} kg	Moon=1	g/cm^3	
Europa	3138	0.84	1.30	0.48	0.65	2.97	0.348[a]
Ganymede	5268	1.41	1.42	1.48	2.00	1.94	0.311[b]
Callisto	4806	1.28	1.24	1.08	1.46	1.86	0.358[c]
Titan	5150	1.37	1.35	1.34	1.81	1.88	?
Triton	2710	0.72	0.77	0.21	0.28	2.05	?
Generic	5000	1.34	1.33	1.24	1.67	1.90	-

[a] *Anderson et al.* [1998b].
[b] *Anderson et al.* [1996].
[c] *Anderson et al.* [1998a].

temperature. For instance, the model of *Friedson and Stevenson* [1983] computes values of the Rayleigh number as a function of the viscosity of the well-mixed interior. The temperature difference across the upper thermal boundary layer is calculated assuming that the system adjusts the total temperature difference ΔT in order to maximize the convective heat flux. For a body like Ganymede they find that ΔT is of the order of 60 K. To compute the heat flux, they apply scaling laws for isoviscous fluid.

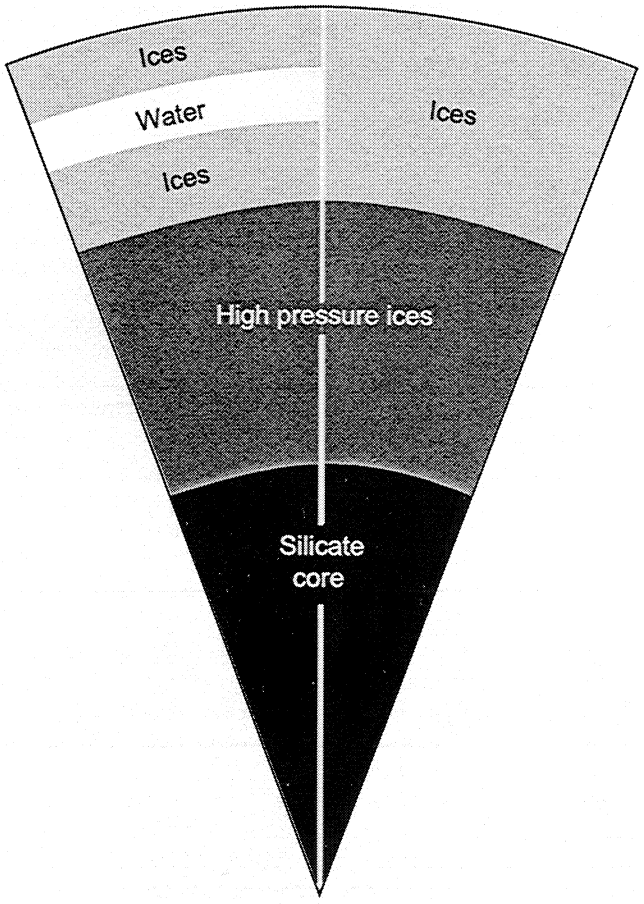

Figure 1. Two possible models for the radial structure of large icy satellites. (right) Heat transfer in the outer layer is efficient enough to transport all of the heat to the surface. The initial ocean has completely crystallized. (left) The outer shell is not able to release all of the heat outward. A residual ocean is still present below the outer shell. Note that Ganymede and Europa may have also differentiated in a metallic core.

However, scaling laws derived from numerical models with strongly temperature-dependent viscosity differ significantly from isoviscous scaling laws [e.g., *Moresi and Solomatov*, 1995; *Dumoulin et al., 1999*; *Deschamps and Sotin*, 2000]. When applied to icy satellites, they predict temperature differences across the thermal boundary layer of the order of 15 K instead of 60 K (see section 2.4). The present study uses one scaling law to calculate the heat flux and a second scaling law to compute the temperature of the well-mixed interior. These scaling laws are based on a recent numerical model of convection including large viscosity variations [*Deschamps and Sotin*, 2000].

Some of the rheological parameters, as well as the deformation process of ice within icy satellites, are only poorly constrained. Assuming that the outer ice shell behaves as a Newtonian fluid, we have constructed several models, depending on the values of the rheological parameters. The efficiency of convection and the possible structure of the satellite are discussed as a function of these values.

Chemical thermodynamic models suggest that volatiles may condense along with water ice in the protoplanetary nebula of gaseous planets [*Lunine and Stevenson*, 1982; *Prinn and Fegley*, 1989]. The presence of volatiles decreases the value of the liquidus at a given depth [e.g., *Sotin et al.*, 1998], and therefore the composition of the initial ocean is an important parameter. Considering that the ice I layer is equivalent to an isoviscous fluid covered by a rigid cap, *Grasset and Sotin* [1996] have shown that in the case of an ammonia-rich ocean, the Rayleigh number reaches a maximum value at a given thickness. The results presented below include the effect of a temperature-dependent viscosity. We find that ammonia, if it is present, significantly reduces the convective strength and is able to stop the crystallization of the ocean.

The first part of this paper outlines some previous results on thermal convection with strong viscosity variations. These results are then applied to the outer layer of icy satellites. In the second part we consider the influence of physical (mean density and radius) and rheological (activation energy and reference viscosity) parameters as well as the composition of the initial ocean. The final section discusses the structure of the satellite as a function of some possible values for these parameters.

2. Numerical Models

The evolution of the structure of large icy satellites is usually based on models of heat transfer through the outer ice I layer [e.g., *Reynolds and Cassen*, 1979; *Cassen et al.*, 1981; *Grasset and Sotin*, 1996]. *Reynolds and Cassen* [1979] have shown that

thermal convection is very likely to occur in this layer. Moreover, they pointed out that heat transfer is efficient enough to complete the crystallization of the initial ocean in a short time (~5×10^8 years). Such models compute new values of the bottom temperature T_1, of the temperature and viscosity of the well-mixed interior (T_c and μ_c), and of the Rayleigh number Ra at each time step. To complete each time step, one needs a relation between the heat flux and the vigor of convection. Scaling laws for an isoviscous fluid were first proposed by *Schubert et al.* [1979]:

$$Nu = a \times Ra^{1/3}, \quad (1)$$

where Nu is the Nusselt number and a is a geometrical parameter. Following the study of *Davaille and Jaupart* [1993], *Grasset and Sotin* [1996] have considered an isoviscous fluid covered by a rigid lid to compute the evolution of Titan. In that case they showed that a pure water ocean crystallizes rapidly. However, the scaling law for a temperature-dependent viscosity differs significantly from (1). Moreover, in the case of a fluid heated from below, the characteristics of the convective sublayer are different from those of an isoviscous fluid [*Deschamps and Sotin*, 2000].

2.1. Scaling Laws for a Temperature-Dependent Viscosity Fluid

Variable viscosity convection has been studied experimentally as well as numerically during the last two decades [e.g., *Nataf and Richter*, 1982; *Christensen, 1984*; *Ogawa et al.*, 1991; *Davaille and Jaupart*, 1993; *Moresi and Solomatov*, 1995]. The flow pattern is highly sensitive to viscosity variations [*White*, 1988]. For instance, if the viscosity is strongly temperature-dependent and convection is not too vigorous, a quasi-stagnant lid develops at the top of the fluid, and convection is confined in a sublayer [e.g., *Davaille and Jaupart*, 1993; *Moresi and Solomatov*, 1995]. In the stagnant lid, heat is transported by conduction. Therefore the heat transfer across the whole fluid is less efficient than in the case of an isoviscous fluid. The convective sublayer consists of cold sinking downwelling, hot rising plumes, thermal boundary layers (TBL), and a nearly adiabatic well-mixed interior. The hot plumes and the lower TBL are present only if the fluid is heated from below. This structure is sketched in Figure 2, in the case of a two-dimensional (2-D) Cartesian fluid.

For a volumetrically heated fluid, there is only one TBL. In that case, laboratory experiments carried out by *Davaille and Jaupart* [1993] show that the temperature difference across the TBL (ΔT_e) is proportional to a "viscous" temperature scale (ΔT_v) defined by

$$\Delta T_v = -\frac{\mu(T_c)}{\left.\frac{d\mu}{dT}\right|_{T=T_c}} \Delta T \quad (2)$$

$$\Delta T_e = 2.24 \Delta T_v, \quad (3)$$

where T_c is the temperature of the well-mixed interior. Moreover, the behavior of the convective sublayer is similar to that of an isoviscous fluid. The 2-D numerical work of *Grasset and Parmentier* [1998] and the 3-D numerical work of *Choblet and Sotin* [2000] agree with these results.

In the case of a bottom heated fluid, a second TBL is present at the bottom. Compared to the isoviscous case (equation (1)), the

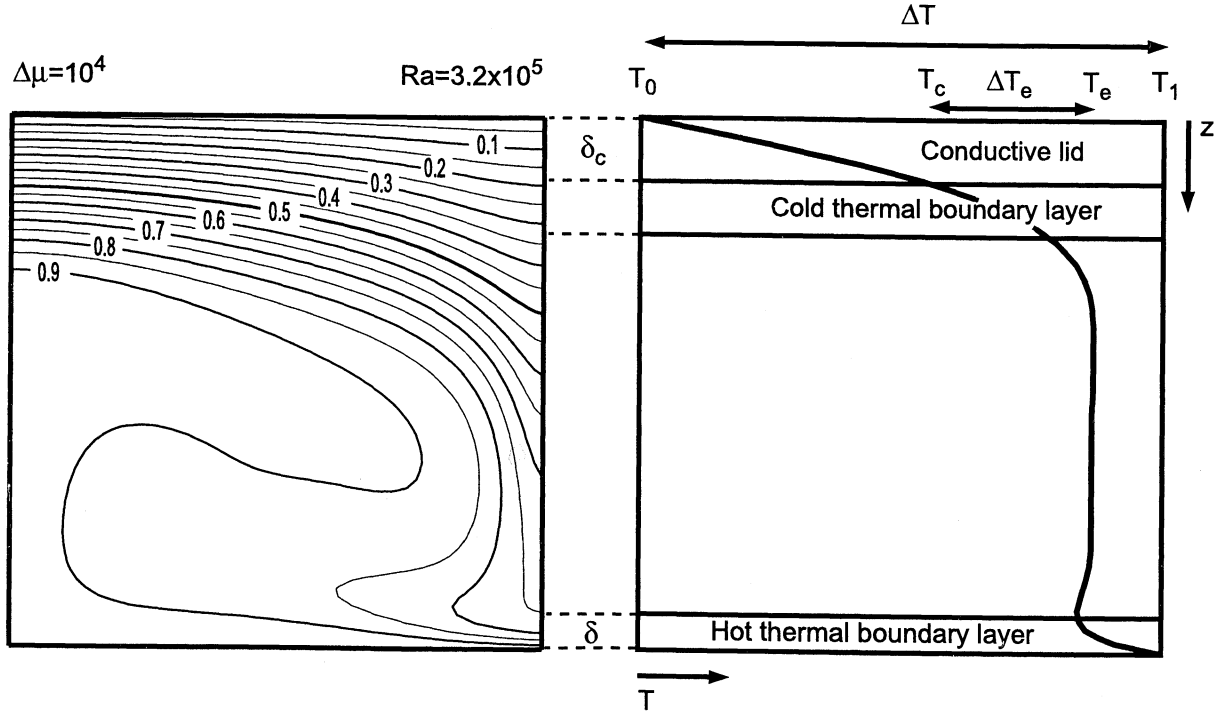

Figure 2. Thermal convection within a strongly temperature-dependent viscosity fluid. A rigid and conductive lid develops at the top of the fluid. (left) In the thermal field, non-dimensional values of the isotherm are indicated with an interval of 0.1. (right) In the thermal profile, T_0 is surface temperature, T_1 is the bottom temperature, T_c is the temperature of the well-mixed interior, and T_e is the temperature at the bottom of the conductive lid. Therefore the temperature difference across the thermal boundary layer is $\Delta T_e = (T_c - T_e)$. In this example the core Rayleigh number is equal to 3.2×10^5, and the top to bottom viscosity ratio is $\Delta\mu = 10^4$.

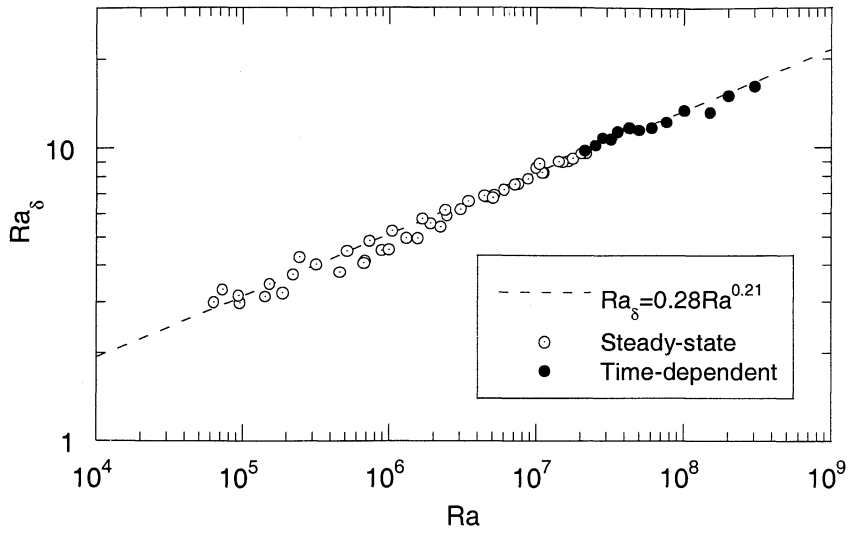

Figure 3. Scaling law for the thermal boundary layer Rayleigh number (Ra_δ) as a function of the core Rayleigh number (equation (8)). The numerical model and computations have been presented in a previous study [*Deschamps and Sotin*, 2000].

determination of the convective heat flux requires not only knowledge of the Rayleigh number but also that of an additional parameter which accounts for viscosity variations [*Christensen*, 1984; *Morris and Canright*, 1984]. Moreover, it is useful to consider the core Rayleigh number defined with the viscosity of the well-mixed interior

$$Ra = \frac{\alpha\rho g \Delta T b^3}{\mu_c \kappa}, \tag{4}$$

where α, ρ, and κ are the coefficient of thermal expansion, the density, and the thermal diffusivity of the fluid, respectively, b and ΔT are the thickness of the fluid layer and temperature difference across this layer, g is the acceleration of gravity, and μ_c is the viscosity of the well-mixed interior. A parameter that accounts well for viscosity variations is [*Morris and Canright*, 1984]

$$\gamma = \frac{\Delta T}{\Delta T_v}, \tag{5}$$

where ΔT_v is defined by (2).

Numerical experiments, which are described by *Deschamps and Sotin* [2000], are carried out in a fluid with a strongly temperature-dependent viscosity. For each experiment the conservative equations of momentum, mass, and energy were solved for a 2-D Cartesian fluid, assuming the Boussinesq approximation and an infinite Prandtl number. The fluid is heated from below, and internal generation of energy is neglected. The viscous law is exponential. Consequently, the viscosity ratio between the top and lower boundary layer is given by

$$\Delta\mu = \exp(\gamma). \tag{6}$$

The numerical experiments described by *Deschamps and Sotin* [2000] suggest that convection is mainly controlled by the bottom TBL. Therefore, in the present study (section 2.4) we propose to compute the heat flux using the thermal boundary layer Rayleigh number Ra_δ:

$$Ra_\delta = \frac{\alpha\rho g \delta T \delta_{TBL}^{\ 3}}{\mu_c \kappa}, \tag{7}$$

where δ_{TBL} is the thickness of the thermal boundary layer and δT is the temperature difference across it. For an isoviscous fluid the value of the thermal boundary layer Rayleigh number depends very little on the Rayleigh number. Its value is close to 10 for both the lower and upper boundary layers [*Bergholz et al.*, 1979; *Sotin and Labrosse*, 1999]. For a temperature-dependent viscosity with two isothermal horizontal boundaries, numerical results [*Deschamps and Sotin*, 2000] suggest that the dependence of the lower thermal boundary layer Rayleigh number upon the core Rayleigh is described by (Figure 3)

$$Ra_\delta = 0.28 Ra^{0.21}. \tag{8}$$

The nondimensional temperature difference across the lower TBL depends on parameter γ, as previously suggested by *Morris and Canright* [1984]

$$(1-\theta_c) = \frac{c_1}{\gamma} + c_2, \tag{9}$$

where θ_c is the nondimensional temperature of the well-mixed interior and c_1 and c_2 are two parameters. A simple least squares fit inversion of our data yields c_1 = 1.43 and c_2 = -0.03 [*Deschamps and Sotin*, 2000], whereas *Morris and Canright* [1984] proposed $c_1 \sim 1.0$ and $c_2 = 0$ on the basis of their analytical work. A possible explanation for this discrepancy is that *Morris and Canright*'s [1984] model does not consider the interaction between hot plumes which rise from the bottom TBL and the conductive lid. It is important to note that the hot plumes interact with the stagnant lid, so that this lid is thermally eroded. Consequently, the limit between the top TBL and the stagnant lid cannot be determined using a viscous temperature scale, as *Davaille and Jaupart* [1993] and *Grasset and Parmentier* [1998] did for a volumetrically heated fluid.

Scaling laws (8) and (9) were built using results of stationary convection with Rayleigh number smaller than 2×10^7. In the ice I layer of icy satellites the Rayleigh number can be as high as 10^9. For such values of the Rayleigh number, convection is usually time-dependent. However, time-average solutions of nonstationary convection also fit well along scaling laws (8) and (9) [*Deschamps and Sotin*, 2000]. Moreover, additional

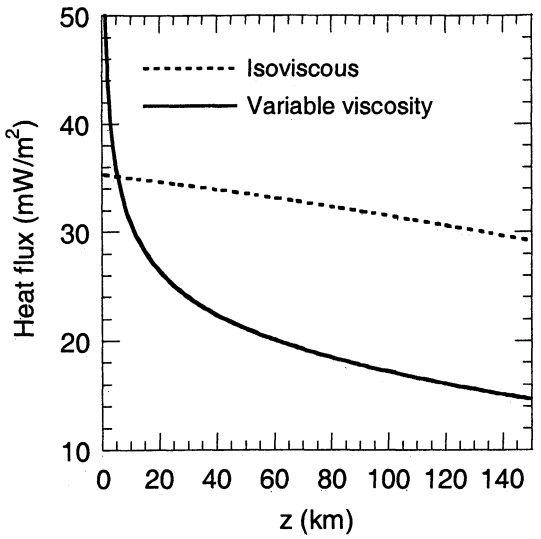

Figure 4. Heat flux as a function of the outer layer's thickness z. For the dotted curve the heat flux is computed with isoviscous scaling laws, i.e., $Nu = 0.294Ra^{1/3}$ and $T_c = \Delta T/2$, where ΔT is the temperature difference between the bottom of the layer and the surface, and T_c is the temperature of the well-mixed interior. For the solid curve the heat flux is computed using equations (18) and (20) (see text), which derive from variable viscosity laws (9) and (8). In both cases the viscosity of the well-mixed interior is given by equation (11), with $E = 60$ kJ/mol and $\mu_0 = 5\times10^{13}$ Pa s.

calculations with Rayleigh number ranging between 5×10^7 and 5×10^8 (solid circles in Figure 3) are in good agreement with these relations.

Scaling relations have also been constructed for non-Newtonian fluids [e.g., *Dumoulin et al.*, 1999; *Reese et al.*, 1999]. The strain rates $\dot{\varepsilon}$ relevant to subsolidus convection within icy satellites are very low: $\dot{\varepsilon} \le 10^{-11}$ s^{-1}. The creep mechanism driving plastic deformation at such strain rates is not very well known and will be discussed below (section 2.2). Since *Dumoulin et al.* [1999] show that non-Newtonian behavior can be accounted for by using a Newtonian creep law with a modified activation energy, scaling relations (8) and (9) are used to parameterize surface heat flux and temperature of the well-mixed interior.

To illustrate the necessity of using variable viscosity scaling laws, we have compared the heat flux predicted by relations (8) and (9) together with that predicted by isoviscous scaling laws. In both cases, the viscosity is computed by (11) (see below), so that the Rayleigh number is computed with the viscosity of the well-mixed interior. The results are presented as a function of the thickness z of the ice I layer (Figure 4). For ice layers thicker than $z = 10$ km, the heat flux predicted by isoviscous scaling laws is overestimated, compared to the heat flux computed by relations (8) and (9). This difference reaches a factor of 2 for a $z = 100$ km thick ice layer.

2.2. Viscosity of Ice I

Considering the results of laboratory experiments, *Durham et al.* [1997] suggested that ice I follows three different flow regimes, depending on the temperature range. Each of these regimes is non-Newtonian, with a stress exponent $n = 4$ ($n = 6$ for the coldest regime). However, the experiments reported by *Durham et al.* [1997] were performed for large grain size, with diameters in the range $0.6 \le d \le 1.0$ mm. For finer grain size material ($3 \le d \le 90$ μm), *Goldsby and Kohlstedt* [1997] showed that the deformation is controlled by grain boundary sliding, with a smaller stress exponent ($n = 1.8$ and $n = 2.4$). Moreover, small values of the strain rate $\dot{\varepsilon}$ favor diffusional creep [e.g., *Goodman et al.*, 1981]. In laboratory experiments the strain rate is seldom smaller than $\dot{\varepsilon} = 10^{-8}$ s^{-1}. However, one expects that strain rates in icy satellites are slower than this value by at least 2 or 3 orders of magnitude. Indeed, measurements performed on mountain glaciers, which are the closest equivalent one can find on Earth, yielded that the strain rate is only slightly stress-dependent, with $n = 1.5$ [*Gerrard et al.*, 1952]. We will then consider the ice I layer of icy satellites as a Newtonian fluid.

The viscosity of ice I depends on the temperature T, and to a lesser extent, on the pressure p. For a Newtonian fluid it is given by

$$\mu(T) = D\exp\left(\frac{E+pV}{RT}\right), \tag{10}$$

where E is activation energy, V is activation volume, and D is a constant. One can also account for pressure dependence by introducing the melting temperature T_m, since this temperature depends on the pressure. A possible law for the viscosity is then

$$\mu(T) = \mu_0 \exp\left[A\left(\frac{T_m}{T}-1\right)\right] \quad A = E/RT_m, \tag{11}$$

μ_0 being a reference viscosity at $T = T_m$. *Weertman* [1968] pointed out that the law (11) provides a good fit of the experimental data and is numerically equivalent to (10). Previous studies have used this kind of law, taking $A = 25$ [*Schubert et al.*, 1981; *Friedson and Stevenson*, 1983].

To estimate the value of the reference viscosity, we have used the results of *Gerrard et al.* [1952]. They measured the strain rate of an alpine glacier for temperatures close to the melting point. For values of the stress between 0.1 and 1.0 bar, they deduced

$$\dot{\varepsilon} = 3\times10^{-16}\sigma^{1.5}, \tag{12}$$

where σ is in Pascals. Again, the strain rate relevant to convection in icy satellites may be smaller than those measured by *Gerrard et al.* [1952] by 1 or 2 orders of magnitude. Assuming that the effective viscosity is given by $\mu = \sigma/2\dot{\varepsilon}$, the viscosity of ice I near the melting point is approximately $\mu_0 = 5\times10^{13}$ Pa s for $\dot{\varepsilon} = 10^{-11}$ s^{-1}. *Goldsby and Kohlstedt* [1997] have performed their experiments at temperatures well below the melting point, yet we have also used their data, and we have found values of the reference viscosity around 10^{13} Pa s. For strain rates lower than and grain sizes larger than those considered by *Goldsby and Kohlstedt* [1997], the reference viscosity should be larger, around 10^{14} Pa s. On the whole, the reference viscosity is not very well constrained. We will assume $\mu_0 = 5\times10^{13}$ Pa s as a reference value and will consider the effects induced by possible variations of 1 order of magnitude around this value.

One must also estimate the value of the activation energy E. The intermediate flow regime proposed by *Durham et al.* [1997] yields a value of E equal to 60 kJ/mol. *Goldsby and Kohlstedt* [1997] deduced very similar values from their experiments. They found $E = 49$ kJ/mol and $E = 55$-62 kJ/mol for a stress exponent equal to $n = 1.8$ and $n = 2.4$, respectively. Moreover, the activation energy of the hydrogen and oxygen atomic diffusion in ice I is close to 60 kJ/mol [*Weertman*, 1983]. Therefore the value of the activation energy yields probably in the range 50-60 kJ/mol. Many previous studies assumed $E = 60$ kJ/mol [e.g.,

Friedson and Stevenson, 1983; *Mueller and McKinnon*, 1988; *Grasset and Sotin*, 1996].

Another reason for investigating a large range of activation energies is to account for possible non-Newtonian behavior. For a stress exponent equal to 3, *Dumoulin et al.* [1999] show that the convective heat flux is identical to that obtained for a Newtonian fluid (stress exponent equal to 1) with an activation energy divided by a factor 2. Activation energy for non-Newtonian deformation is around 90 kJ/mol [*Durham et al.*, 1997]. Non-Newtonian deformation can be accounted for by using an activation energy equal to 45 kJ/mol.

2.3. Liquidus of Water

To compute the reference viscosity, one needs to know the temperature at the bottom of the ice layer (T_1). Moreover, the temperature of the well-mixed interior depends on T_1 (section 2.4, equation (18)). By definition, T_1 is equal to the value of the water liquidus (T_m) at a depth equal to the thickness of the ice layer. Obviously, the liquidus depends strongly on the composition of the initial ocean. Here we have considered the liquidus of a mixture of ammonia (NH_3) and water.

For pure water we have used the relationship proposed by *Chizhov* [1993]. This liquidus reaches a minimum value at a pressure of p = 0.207 GPa, which corresponds to a depth of ~170 km in the case of the large icy satellites. Between p = 0 and p = 0.207 GPa, this liquidus fits well along the curve

$$T_m = 273.2\left(1-\frac{p}{0.395}\right)^{1/9}. \quad (13)$$

Note that the shape of the liquidus implies that the ocean freezes simultaneously at its top and at its bottom.

The liquidus of water is very sensitive to the presence of volatiles, such as ammonia and methane. The phase diagram of the ammonia-water system is relatively well documented [e.g., *Johnson and Nicol*, 1987; *Boone and Nicol*, 1991; *Grasset et al.*, 1995; *Hogenboom et al.*, 1997]. The melting temperature at a given pressure increases as the amount of ammonia increases [e.g., *Sotin et al.*, 1998]. As long as the ammonia ratio (x_{NH3}) is lower than 32.1%, pure water crystallizes alone and ammonia remains in the residual liquid. On the other hand, if x_{NH3} > 32.1%, ammonia dihydrate crystallizes. *Grasset et al.* [1995] measured the liquidus of a solution with 15% ammonia up to a pressure of 1.5 GPa. In the stability field of ice I the melt temperature is well described by

$$T_m = 253.0 - 85.1p - 281.1p^2. \quad (14)$$

Hogenboom et al. [1997] performed experiments for pure dihydrate (x_{NH3} = 32.1%). Up to a pressure of 0.3 GPa the melting temperature is analytically approached by

$$T_m = 176.3 + 24.3p - 77.6p^2. \quad (15)$$

A pure ice I layer forms at the top of the deep ocean, whereas ammonia remains in the ocean. Thus the ammonia ratio increases as the ice I layer thickens. In our calculations, (13)-(15) are used to extrapolate the melt temperature for a given pressure and a given ammonia ratio.

2.4. Outline of the Calculations

Most of our results are presented as a function of the thickness of the outer ice I layer (z). First, for a given value of z we compute the pressure p and the value of the liquidus at this pressure (T_m). By definition, the temperature at the bottom of the convective layer (T_1) is equal to T_m. The surface temperature T_0 is an input datum and we call ΔT the difference between the bottom and surface temperatures. Note that because T_1 depends on z, ΔT is also depth-dependent.

The temperature of the well-mixed interior (T_c) is given by the dimensional form of the scaling law (9)

$$T_c = T_1 - \Delta T\left(\frac{c_1}{\gamma}+c_2\right). \quad (16)$$

According to *Davaille and Jaupart* [1993], and if one considers the viscosity law (11), the parameter γ is

$$\gamma = \frac{E\Delta T}{RT_c^2}. \quad (17)$$

Substituting relation (17) into (16), T_c is defined by a polynomial of degree 2. The positive root of this polynomial is

$$T_c = B\left[\sqrt{1+\frac{2}{B}(T_1 - C)}-1\right] \quad B=\frac{E}{2Rc_1},\ C=c_2\Delta T. \quad (18)$$

We also compute the viscosity of the well-mixed interior (μ_c), using law (11). As previously mentioned, the constant μ_0 is the viscosity of ice I close to the liquidus at depth z. In other words, μ_0 is the viscosity at the bottom of the convective layer.

The core Rayleigh number is then computed with (4), where we have replaced the thickness of the fluid layer b with z, and α, ρ, and κ with the properties of ice I (α_I, ρ_I and κ_I, see Table 2 for definitions and values). The acceleration of gravity at the surface of the satellite (g) typically yields in the range 1.2-1.4 m/s^2. From

Table 2. Properties of Ice I and Possible Values of the Rheological Parameters μ_0 and E

Physical Quantity	Symbol	Unit	Value	Reference
Density	ρ_I	kg/m^3	917	*Hobbs* [1974]
Thermal conductivity	k_I	W/m/K	2.6	*Hobbs* [1974]
Thermal diffusivity	κ_I	m^2/s	1.47×10^{-4}	*Hobbs* [1974]
Coefficient of thermal expansion	α_I	K^{-1}	1.56×10^{-4}	*Hobbs* [1974]
Latent heat	L_I	kJ/kg	284	*Kirk and Stevenson* [1987]
Viscosity at the melting point	μ_0	Pa s	5×10^{13}	*Gerrard et al.* [1952][a]
Activation energy	E	kJ/mol	50-60	*Goldsby and Kohlstedt* [1997]

[a] the reference viscosity is estimated from flow measurements on an alpine glacier.

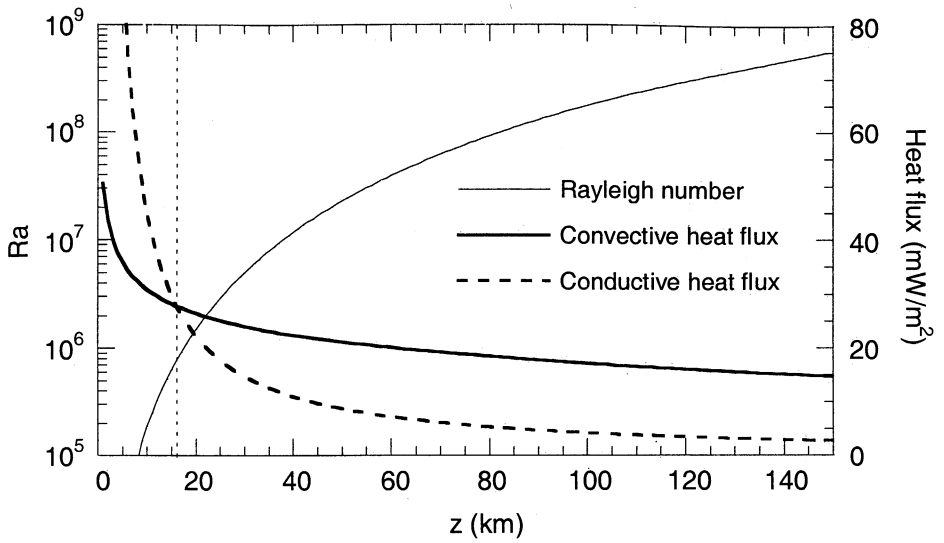

Figure 5. Rayleigh number (solid thin curve) and convective heat flux (solid thick curve) as a function of the outer layer's thickness z, in the case of a generic satellite ($<\rho> = 1.9$ g/cm^3 and $R = 2500$ km). The surface temperature is $T_0 = 100$ K. The conductive heat flux (dashed thick curve) is shown for comparison. The rheological parameters are $\mu_0 = 5\times10^{13}$ Pa s and $E = 60$ kJ/mol. Convection is possible if $z > 17$ km (dotted vertical line). The Rayleigh number increases with z, whereas the heat flux decreases as a consequence of the stagnant lid.

(8), we compute the value of the lower thermal boundary layer Rayleigh number Ra_δ. The thickness of the lower thermal boundary layer (δ) and the heat flux at the bottom of the ice layer (Φ_{bot}) are given by

$$\delta = \left[\frac{\mu_c \kappa_I}{\alpha_I \rho_I g (T_1 - T_c)} Ra_\delta\right]^{1/3} \quad (19)$$

$$\Phi_{bot} = \frac{k_I (T_1 - T_c)}{\delta}, \quad (20)$$

respectively, where k_I is the thermal conductivity of ice I (Table 2). Because we have assumed that there is no internal heating, energy balance implies that the heat flux is constant through the whole ice layer and is equal to the bottom heat flux. Therefore (20) is also the convective heat flux at the top of an ice layer of thickness z (q_{surf}). Note that the heat transferred by subsolidus convection decreases with increasing value of the ice layer thickness.

Finally, we have computed the thickness of the thermal lithosphere (e_{th}). The thermal lithosphere is the layer through which heat is transferred by conduction. It is defined by the addition of the top thermal boundary layer and of the conductive lid:

$$e_{th} = \frac{k_I (T_c - T_0)}{q_{surf}}, \quad (21)$$

where q_{surf} is the heat flux at the surface and is given by (20). It is also useful to estimate the thickness of the mechanical lithosphere. The bottom of this lithosphere is usually defined by the isotherm (T_{lith}), so that

$$e_{mech} = \frac{k_I (T_{lith} - T_0)}{q_{surf}}, \quad (22)$$

where T_{lith} is the temperature at which the deformation of ice becomes ductile instead of brittle. This temperature depends on parameters such as strain rate and shear stress, and different values have been investigated.

3. Results

3.1. The "Generic" Satellite

First, let us use the approach of *McKinnon* [1998] and define a "generic" satellite, that is to say, a satellite whose physical properties are close to the mean values of the physical properties of the large icy satellites. The radius R of the largest icy satellites (i.e., Callisto, Titan, and Ganymede) varies between 2400 and 2600 km, whereas their mean density $<\rho>$ yields in the range 1.86-1.94 g/cm^3 (Table 1). Therefore the generic satellite has a radius $R = 2500$ km and a mean density $<\rho> = 1.9$ g/cm^3. Note that these values are close to those of Titan. We assume a surface temperature T_0 equal to 100 K. Additional results of our model (not shown here) suggest that this parameter is not influent. Following the discussion of section 2.2, we assumed that the activation energy and the reference viscosity of ice I are equal to 60 kJ/mol and 5×10^{13} Pa s, respectively. Finally, the initial ocean is made of pure water. In other words, the generic satellite can be used as a reference to study the physical, rheological, and compositional parameters.

In Figure 5, we have plotted the core Rayleigh number (solid thin curve) and the convective heat flux (solid thick curve) as a function of the thickness of the ice I layer (z). The thickness of the ice I layer at the onset of convection (z_c) is equal to 17 km. Then, convection becomes more vigorous as the layer thickens. The minimum value of the liquidus ($T_1 = 251$ K at $p = 0.207$ GPa) is reached for a 170 km thick layer. Consequently, the temperature of the well-mixed interior (equation (18)) also decreases as the ice layer thickens. The parameter γ (equation (17)), which measures the relative importance of the stagnant lid, increases slightly with the thickness of the ice layer: it varies from $\gamma = 17.9$ for $z = 17$ km to $\gamma = 18.2$ for $z = 150$ km. In the

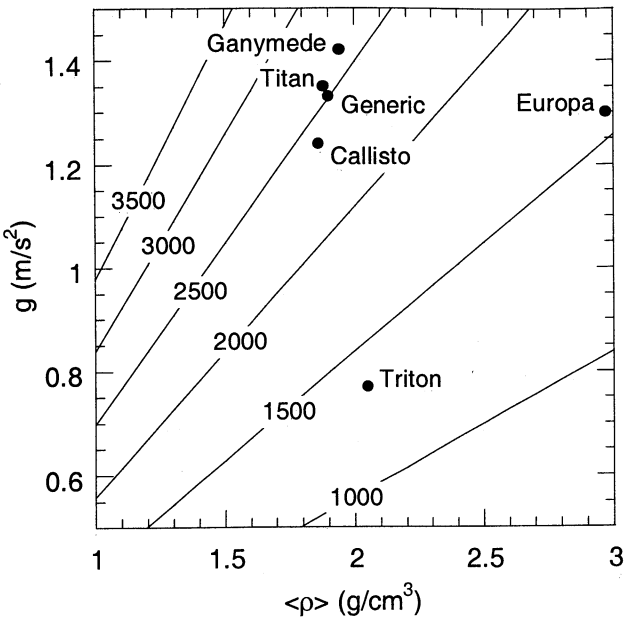

Figure 6. Acceleration of gravity as a function of the mean density for several values of the radius. The value of the radius in kilometers is indicated on each line. For comparison, we have located the main icy moons as well as the hypothetical generic satellite. Note that the icy moons of Jupiter have approximately the same acceleration of gravity. Triton has a smaller acceleration of gravity owing to a smaller radius.

range $17 \le z \le 170$ km the Rayleigh number yields in the interval 10^6-10^{10}, and therefore convection remains in the stagnant-lid regime.

One can see that the heat flux decreases as the layer thickens. For instance, the heat flux at the onset of convection is equal to 27.4 mW/m^2, whereas the heat flux for a 150 km thick layer is equal to only 14.7 mW/m^2. The decrease of the heat flux is due to the thickening of the conductive lid. One can note that the nondimensional heat flux (Nusselt number) increases with increasing values of the Rayleigh number but that its value is limited by the thickness of the stagnant lid. On the other hand, the conductive heat flux (Φ_c, dashed thick curve in Figure 5) decreases as the thickness of the layer increases. The decrease of Φ_c is more important than the increase of the Nusselt number, and on the whole, the convective heat flux decreases as the ice layer thickens.

In order to investigate the effect of rheological and compositional parameters, it is interesting to define a mean heat flux <Φ> between two values of the thickness of ice I (z_1 and z_2):

$$<\Phi> = \frac{1}{(z_2 - z_1)} \int_{z_1}^{z_2} \Phi(z) dz \,. \tag{23}$$

For example, the value of <Φ> for the generic satellite is equal to 19.1 mW/m^2 between z_1 = 17 km (onset of convection) and z_2 = 150 km (pressure of the triple point ice I-ice III-water).

3.2. Physical Parameters (<ρ>, *R*)

The effects induced by the variations of the mean density <ρ> and of the radius R are now investigated. If one considers planetary bodies like Callisto (<ρ> = 1.86 g/cm^3 and R ~ 2400 km) or Ganymede (<ρ> = 1.94 g/cm^3 and R~2600 km), the variations of g remain small (around 7% of the generic value), and the convection in the outer shell would not change significantly. On the other hand, one expects larger differences in the case of smaller satellites such as Triton (<ρ> = 2.05 g/cm^3 and R ~ 1350 km), the largest moon of Neptune. Actually, it is more relevant to consider the variations of the surface acceleration of gravity g. Indeed, any variations of g induce a variation of the Rayleigh number and shift the depth of the liquidus. Moreover, the variations of g are equivalent to <ρ> and R variations since:

$$g = \frac{4}{3} \pi G <\rho> R \tag{24}$$

The generic value of g is equal to 1.33 m/s^2. Observed values in the solar system are listed in Table 1. In Figure 6, g is plotted as a function of the mean density and for several values of the radius.

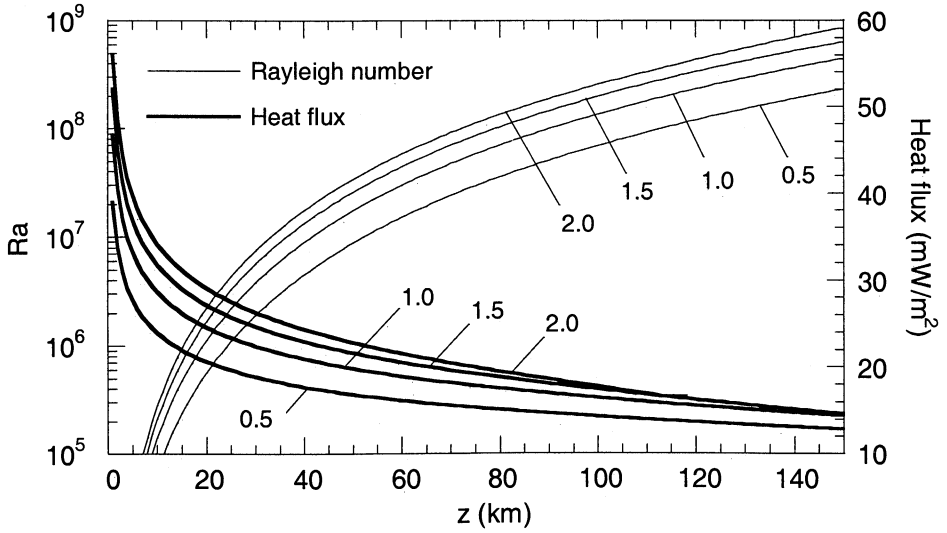

Figure 7. Rayleigh number (thin lines) and heat flux (thick lines) as a function of the total thickness of the ice I layer and for different values of the gravity acceleration. The numbers on each curve indicate the value of the acceleration of gravity in m/s^2. E = 60 kJ/mol and $\mu_0 = 5 \times 10^{13}$ Pa s.

Table 3. Influence of the Acceleration of Gravity g[a]

g, m/s^2	z_c, km	$\Phi(z_c)$, mW/m^2	$<\Phi>$, mW/m^2
0.50	24.0	19.9	15.4
0.75	21.0	22.7	17.0
1.00	19.0	24.9	18.1
1.25	18.0	26.7	18.9
1.50	17.0	28.2	19.4
2.00	15.0	31.2	20.6

[a] z_c is the critical thickness for the onset of convection, $\Phi(z_c)$ is the heat flux at the onset of convection, and $<\Phi>$ is the mean convective heat flux between $z = z_c$ and z = 150 km. E = 60 kJ/mol and $\mu_0 = 5\times10^{13}$ Pa s.

Table 4. Influence of the Activation Energy E[a]

E, kJ/mol	z_c, km	$\Phi(z_c)$, mW/m^2	$<\Phi>$, mW/m^2
40	11.0	58.8	38.2
50	14.0	39.3	26.6
60	17.0	27.4	19.1
70	21.0	19.5	14.0
80	25.0	14.1	10.4
90	28.0	10.3	7.8

[a] z_c is the critical thickness for the onset of convection, $\Phi(z_c)$ is the heat flux at the onset of convection, and $<\Phi>$ is the mean convective heat flux between $z = z_c$ and z = 150 km. g = 1.33 m/s^2 and $\mu_0 = 5\times10^{13}$ Pa s.

Note that the accelerations of gravity of the largest icy satellites are very close to each other: g = 1.3±0.1 m/s^2. Europa is smaller but has a higher density, so that its acceleration of gravity is close to the generic value. On the other hand, the acceleration of gravity at the surface of Triton is significantly smaller (g = 0.77 m/s^2).

Increasing the acceleration of gravity has two main effects. First, according to (4), the vigor of convection increases. Second, the pressure at a given depth increases. As a consequence of the pressure rise, the liquidus temperature decreases. However, this does not affect the viscosity because the temperature difference across the lower TBL is nearly constant (equation (18)) and the viscosity depends on the ratio of the melting temperature to the temperature of the well-mixed interior (equation (11)).

The influence of the gravity acceleration is shown in Figure 7. We have explored the range $0.5 \leq g \leq 2.0$ m/s^2, assuming $\mu_0 = 5\times10^{13}$ Pa s, E = 60 kJ/mol, and a pure water primordial ocean. The critical thickness for the onset of convection (z_c) does not change significantly: z_c = 24 and 15 km for g = 0.5 and 2.0 m/s^2, respectively (Table 3). Moreover, the Rayleigh number depends only slightly on the gravity (thin lines in Figure 7). Note that for g = 0.5 m/s^2, it is higher than 10^6, whatever the thickness of the ice I layer. Therefore convection remains possible in small and light bodies, such as Triton.

The efficiency of convection increases slightly with g (thick lines in Figure 7), but the differences are not significant in the interval $1.0 \leq g \leq 2.0$ m/s^2. Though they remain small, the differences are more pronounced in the range $0.5 \leq g \leq 1.0$ m/s^2, that is to say, for small and light satellites. For instance, the mean heat flux for g = 0.5 m/s^2 is still 80% of the mean heat flux for g = 1.5 m/s^2.

Thus, the radius and the mean density have only a limited influence on the convection in the outer ice I layer. Variations as large as ΔR = ±1000 km or $\Delta<\rho>$ = ±1.0 g/cm^3 do not induce strong modifications. Convection is possible in the outer layer of small and light satellites, though it is less efficient. This result is in agreement with the study of *McKinnon* [1998].

3.3. Rheological Parameters (E, μ_0)

As discussed above, the activation energy E may be close to 50-60 kJ/mol. However, values in the ranges 40-50 kJ/mol and 60-90 kJ/mol must not be excluded [*Durham et al.*, 1997]. The results presented in Figure 8a and Table 4 were obtained for values of E between 40 and 90 kJ/mol, assuming $\mu_0 = 5\times10^{13}$ Pa s, R = 2500 km and $<\rho>$ = 1.9 g/cm^3. The critical thickness for the onset of convection varies between z_c = 11 km for E = 40 kJ/mol, and z_c = 28 km for E = 90 kJ/mol (Table 4). In a more general way, the Rayleigh number depends very slightly on the activation energy (thin lines in Figure 8a). This is not surprising since both the temperature (T_c, equation (18)) and the viscosity (μ_c, equation (11)) of the well-mixed interior do not depend strongly on E. For example, the value of μ_c for E = 40 kJ/mol is only 1.5 larger than that for E = 90 kJ/mol. Note that since T_c increases slightly with E, the Rayleigh number is slightly higher (~1.5) for E = 40 kJ/mol than for E = 90 kJ/mol. On the other hand, the activation energy controls the amplitude of the viscosity variations (equation (17)): the larger the value of E, the stronger the viscosity variations and the smaller the heat flux. For a given thickness of ice I, the heat flux for E = 90 kJ/mol is only 20% of the heat flux for E = 40 kJ/mol (thick lines in Figure 8a). In addition, the mean heat flux between $z_1 = z_c$ and z_2 = 150 km (equation (23)) is equal to 38.2 mW/m^2 for E = 40 kJ/mol and only 7.8 mW/m^2 for E = 90 kJ/mol (Table 4).

The reference viscosity (μ_0) controls the viscosity of the well-mixed interior. Thus the vigor and the efficiency of convection are decreasing when the viscosity is getting larger (Figure 8b). Moreover, a thicker layer of ice I is needed to reach the onset of convection: the critical thickness is equal to 8 and 37 km for a reference viscosity of 5×10^{12} and 5×10^{14} Pa s, respectively (Table 5). If μ_0 increases by one order of magnitude, the Rayleigh number decreases also by one order of magnitude (thin lines in Figure 8b), and the heat flux is divided by approximately a factor two (thick lines in Figure 8b). The mean heat flux is equal to 36.3 mW/m^2 for $\mu_0 = 5\times10^{12}$ Pa s, whereas it is equal to 9.9 mW/m^2 for $\mu_0 = 5\times10^{14}$ Pa s (Table 5).

Table 5. Influence of the Reference Viscosity μ_0[a]

μ_0, Pa s	z_c, km	$\Phi(z_c)$, mW/m^2	$<\Phi>$, mW/m^2
5×10^{12}	8.0	59.4	36.3
10^{13}	10.0	47.1	30.0
5×10^{13}	17.0	27.4	19.1
10^{14}	22.0	21.5	15.7
5×10^{14}	37.0	12.4	9.9

[a] z_c is the critical thickness for the onset of convection, $\Phi(z_c)$ is the heat flux at the onset of convection, and $<\Phi>$ is the mean convective heat flux between $z = z_c$ and z = 150 km. g = 1.33 m/s^2 and E = 60 kJ/mol.

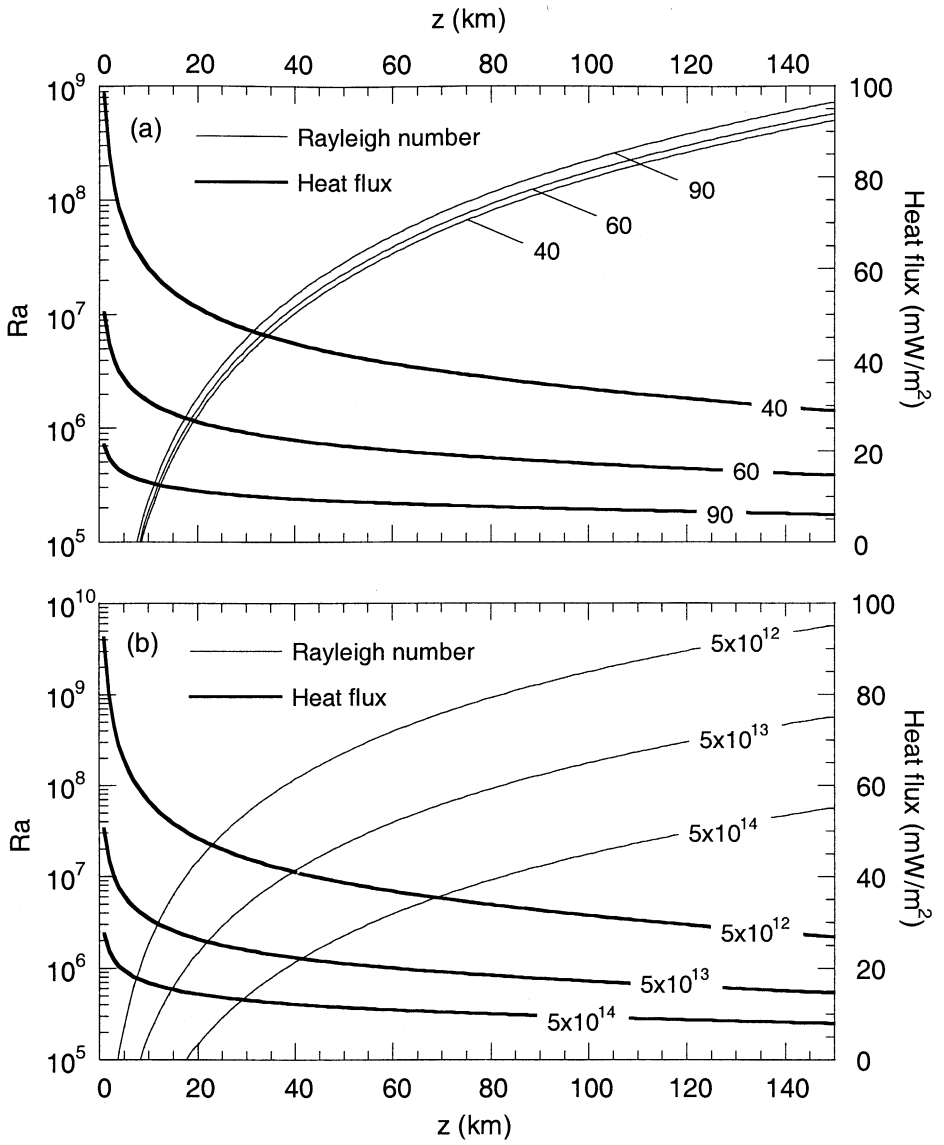

Figure 8. (a) Rayleigh number (thin lines) and heat flux (thick lines) as a function of the total thickness of the ice I layer and for different values of the activation energy (the value of E is indicated on each curve). The reference viscosity is equal to 5×10^{13} Pa s. (b) Same as Figure 8a but for different values of the reference viscosity (the value of μ_0 is indicated on each curve). The activation energy is fixed to 60 kJ/mol. The values of the other parameters are $\langle\rho\rangle = 1.9$ g/cm^3, $R = 2500$ km, and $T_0 = 100$ K for both Figure 8a and Figure 8b.

3.4. Composition of the Initial Ocean

We now consider the possible presence of ammonia in the initial ocean. As the ice I layer thickens, the amount of ammonia increases, and the melting temperature decreases. Consequently, the viscosity of the well-mixed interior increases, and the convection weakens. In the case of an isoviscous ice I layer, the Rayleigh number reaches a maximum value at a given thickness [*Grasset and Sotin*, 1996].

Our computations indicate that this phenomenon also happens in the case of a temperature-dependent viscosity fluid (Figure 9a). The greater the ammonia ratio, the smaller the value of the liquidus at a given pressure, and the less vigorous the convection. In Figure 9a the horizontal dashed line represents the onset of convection. One can see that convection is possible only if the thickness of the ice layer yields between two critical values. The critical thickness for the onset of convection (z_{c1}) increases as the ammonia ratio increases. On the other hand, the critical thickness for the breakdown of convection (z_{c2}) decreases as the ammonia ratio increases. As a result, for $\mu_0 = 5\times10^{13}$ Pa s and $E = 60$ kJ/mol, convection is possible only if the initial amount of ammonia is lower than 12%. For a smaller reference viscosity ($\mu_0 = 5\times10^{12}$ Pa s), convection is possible even for an ocean with 15% ammonia. Similarly, if E is only 40 kJ/mol, a 20-65 km thick ice I layer is unstable even for $x_{NH3} = 15\%$ (Table 6).

The heat flux across the ice I layer is represented in Figure 9b. For a given thickness of the ice layer the heat flux decreases as the amount of ammonia increases: convection is less vigorous and therefore less efficient. Table 6 lists the mean heat flux between the onset and the breakdown of convection for several cases. This heat flux decreases as the ammonia ratio increases: assuming $E = 60$ kJ/mol and $\mu_0 = 5\times10^{13}$ Pa s, the mean heat flux for an ammonia ratio of 5, 8, and 10% is 29, 42, and 50% smaller, respectively, than that for a pure water ocean.

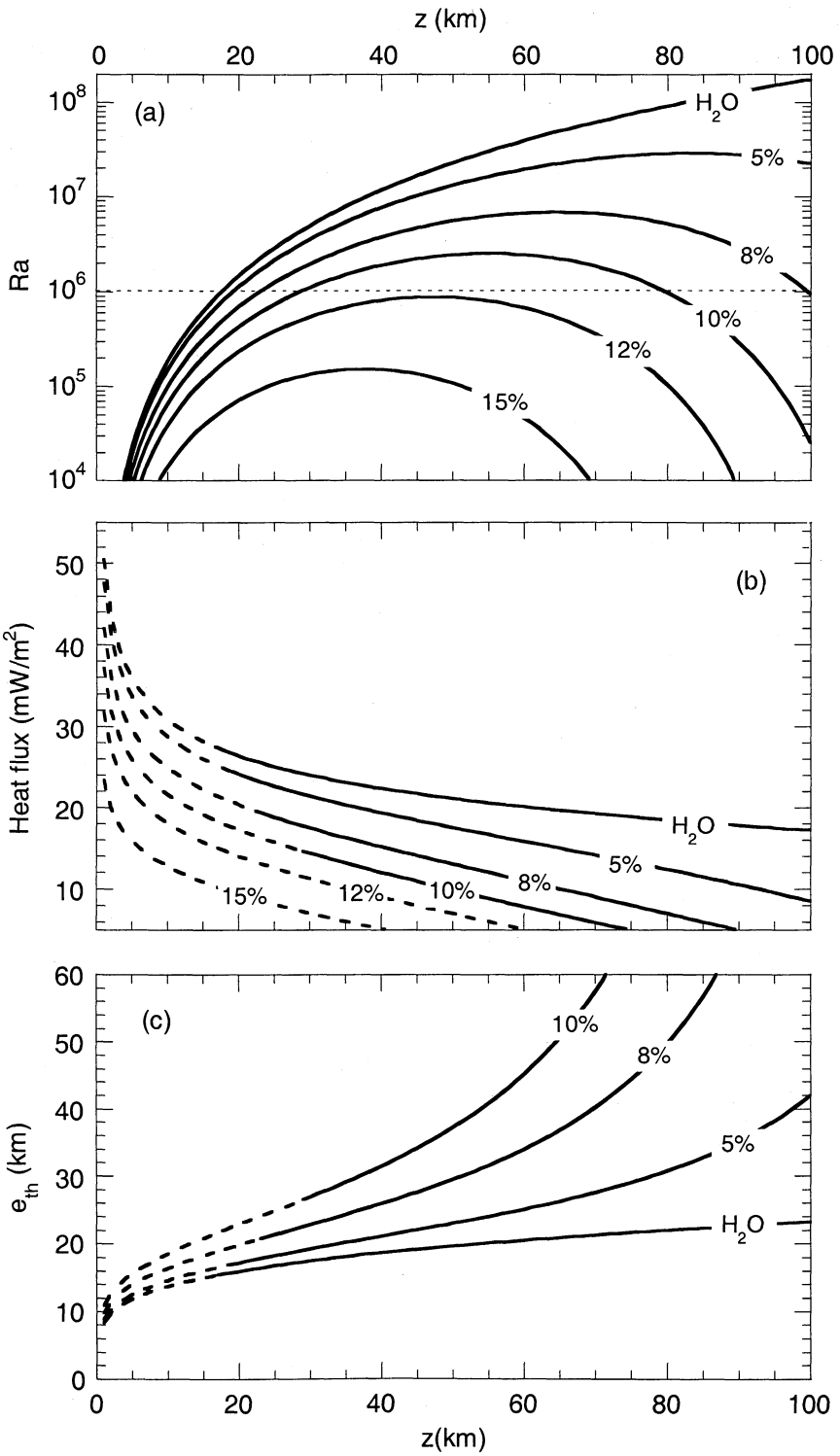

Figure 9. (a) Core Rayleigh number as a function of the thickness of the ice I layer and for several compositions of the initial ocean. The dashed horizontal line indicates the approximate value of the critical Rayleigh number. Below this limit, convection does not occur. (b) Convective heat flux as a function of the thickness of the ice I layer. The dashed sections of the curves mean that the ice I layer does not convect: the calculated heat flux is an extrapolated value. (c) Thickness of the thermal lithosphere as a function of the total thickness of the ice I layer and for different compositions of the initial ocean. The initial ammonia ratio is indicated on each curve. The physical parameters are: $R = 2500$ km, $g = 1.33$ m/s^2, and $T_0 = 100$ K. The rheological parameters are: $E = 60$ kJ/mol and $\mu_0 = 5\times10^{13}$ Pa s.

Figure 9c shows the thickness of the thermal lithosphere (e_{th}, defined by equation (21)) as a function of the total thickness of ice I, assuming $\mu_0 = 5\times10^{13}$ Pa s and $E = 60$ kJ/mol. The thermal lithosphere is the layer formed by the stagnant lid and the top thermal boundary layer. For pure water this thickness is roughly constant around 15 km, independently of the total thickness of the ice I layer. For a given total thickness of the ice layer a small ammonia ratio (e.g., 5%) increases slightly the thickness of the

Table 6. Influence of the Composition of the Initial Ocean[a]

x_{NH3}, %	E, kJ/mol	μ_0, Pa s	z_{c1}, km	z_{c2}, km	$<\Phi>$, mW/m^2
5	60	10^{13}	11	132	21.1
10	60	10^{13}	15	92	14.7
15	60	10^{13}		does not convect	
5	40	5×10^{13}	11	137	28.3
10	40	5×10^{13}	14	102	20.1
15	40	5×10^{13}	23	65	13.6
5	60	5×10^{13}	19	127	13.5
10	60	5×10^{13}	29	79	9.3
15	60	5×10^{13}		does not convect	
5	60	10^{14}	24	124	11.1
10	60	10^{14}	42	67	7.6
15	60	10^{14}		does not convect	

[a] z_{c1} and z_{c2} are the critical thickness at the onset and breakdown of convection, respectively, and $<\Phi>$ is the mean convective heat flux between z_{c1} and z_{c2}. Several values of the rheological parameters (E and μ_0) are considered. R = 2500 km and $<\rho>$ = 1.9 g/cm^3.

lithosphere. On the other hand, for higher values of this ratio (e.g., 10%) the lithosphere is much thicker. Moreover, the thickness of the lithosphere increases as a function of the total thickness of ice I. The higher the value of the ammonia ratio, the more dramatic the increase of the lithosphere thickness.

One wants to point out that it is more relevant to consider the mechanical lithosphere, that is to say, the layer where deformation is brittle rather than ductile. The limit between brittle and ductile deformation is usually defined by an isotherm (T_{lith}). The value of this isotherm is, of course, lower than that of the temperature of the well-mixed interior. Therefore one expects the mechanical lithosphere to be thinner than the thermal lithosphere. The value of this isotherm depends on parameters such as creep activation energy, strain rate, and shear stress. Unfortunately, in the case of icy satellites these parameters are poorly constrained. In Figure 10 we have plotted the thickness of the mechanical lithosphere as a function of the total thickness of ice I for different possible values of the threshold isotherm and an initial ammonia ratio equal to 8%. The thickness of the thermal lithosphere is indicated by the dotted line. The thin solid line represents the lithosphere defined by T_{lith} = 150 K, in the case of a pure water ocean. As expected, the mechanical lithosphere is thinner than the thermal lithosphere: for z = 50 km the lithospheres defined by the isotherms 200, 175, and 150K are thinner than the thermal lithosphere by a factor 1.5, 2.0, and 3.0, respectively. On the other hand, the thickness of the mechanical lithosphere increases strongly as a function of the total thickness of the ice I layer, whatever the value of the isotherm. This feature is similar to that observed for the thermal lithosphere and is controlled by the variations of the convective heat flux.

Therefore the composition of the ocean is a very sensitive parameter. If volatiles are present in this ocean, the vigor and the efficiency of thermal convection decrease significantly, and the lithosphere thickens.

4. Discussion

In a recent study, *Grasset et al.* [2000] showed that in the case of a pure-water ocean, the crystallization of Titan's primordial ocean has probably been completed. On the other hand, they pointed out that a volatile-rich initial ocean inhibits the crystallization. Our model does not include the energetic balance of the outer layer, and therefore it does not provide any time evolution of the structure. However, studying the efficiency of convection as a function of physical, rheological, and compositional parameters leads to some interesting general conclusions. To compute the energy released by a core of silicate of radius r_c, we used the relation proposed by *Kirk and Stevenson* [1987] for the heat flux at the top of the core (Φ_c) as a function of time:

$$\Phi_c(t) = 2\sqrt{\frac{\kappa_c t}{\pi}}\rho_c \sum_i H_i(t), \quad H_i(t) = C_i h_i \frac{1-e^{-\lambda_i t}}{\lambda_i t}. \qquad (25)$$

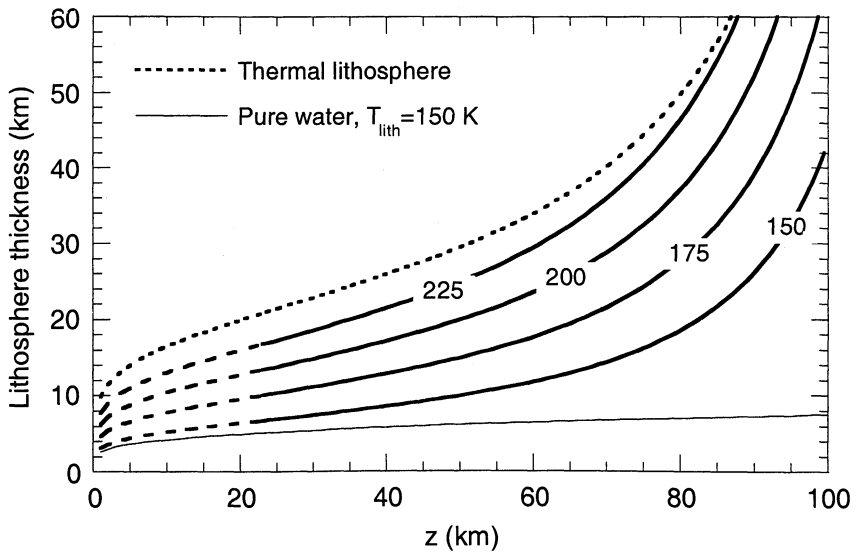

Figure 10. Thickness of the mechanical lithosphere as a function of the total thickness of the ice I layer and for different values of the critical isotherm (indicated on each curve). For comparison, the dotted line represents the thickness of the thermal lithosphere. The thin solid curve corresponds to the thickness of a lithosphere defined by T_{lith} = 150 K in the case of a pure-water ocean. The initial ammonia ratio is equal to 8%. The physical parameters are: R = 2500 km, g = 1.33 m/s^2, and T_0 = 100 K. The rheological parameters are: E = 60 kJ/mol and $\mu_0 = 5\times10^{13}$ Pa s.

Here, ρ_c and κ_c are the density and the thermal diffusivity of silicates, respectively. The power per mass of rock (H_i) radiated by long-lived radioisotopes ^{235}U, ^{238}U, ^{232}Th, and ^{40}K are summed according to the decay constants λ_i, heat release h_i, and initial chondritic abundances C_i of these elements (Table 7). Heat flux at the top of the core reaches a maximum value around 25 mW/m^2 after 2.5 Gyr and then decreases slightly until Φ_c = 24 mW/m^2 at t = 4.55 Gyr. Integrating (25) from t = 0 to t = 4.55 Gyr gives an estimate of the total energy at the bottom of the outer ice layer. For r_c = 1900 km, ρ_c = 3300 kg/m^3, and $\kappa_c = 10^{-6}$ m^2/s this energy is $E_c = 1.5\times10^{29}$ J. The characteristic time of cooling (t_c), that is to say, the time needed to transport the energy E_c through the ice I layer, is approximated by the ratio of E_c to the mean convective heat flux (equation (23)). Assuming a mean thickness of z = 150 km for the ice I layer, t_c is given by

$$t_c = \frac{68.5}{<\Phi>}, \qquad (26)$$

where t_c is expressed in Gyr and $<\Phi>$ is expressed in mW/m^2. To completely release E_c in $t_c \leq$4.55 Gyr, the mean heat flux should be higher than 15.0 mW/m^2. In the remainder of the discussion we will use this value as a reference value.

For a generic satellite with a pure-water primordial ocean, the mean convective heat flux across the outer ice layer and the characteristic time of cooling are equal to 19.1 mW/m^2 and 3.6 Gyr, respectively. Convection is efficient enough to transfer heat toward the surface, and the initial ocean may have crystallized completely. Note, however, that complete crystallization of the initial ocean is not a rapid geological event. The mean density and the radius have only a slight influence on the onset and strength of convection. Convection may occur, or have occurred, in satellites such as Triton (Table 1). On the other hand, variations of the heat flux are more pronounced, and the diminution of the efficiency of convection for low values of g cannot be neglected (Table 3). For example, if g = 0.77 m/s^2, the mean heat flux is equal to 17.0 mW/m^2, and t_c ~ 4.0 Gy.

In the case of complete crystallization it is important to investigate the pattern of convection (layered or single-cell) since several phase transitions may occur (ice I/ice II, ice II/ice V or ice II/ice VI, and ice V/ice VI). The effect of the ice phase transitions on the pattern of convection has been studied by linear stability analysis [*Bercovici et al.*, 1986; *Sotin and Parmentier*, 1989]. The conclusions were that both ice II/iceV and ice II/ice VI transitions inhibit convection and yield a layered pattern. This result was recently confirmed for the ice II/ice VI phase transition by axisymmetric numerical calculations [*Forni et al.*, 1998].

The convective heat flux is very sensitive to the rheology of ice I. However, the viscosity law of ice I in the environment of icy satellites is not well constrained. Considering that the strain rate is very small (~10^{-11} s^{-1}), we have assumed that ice I behaves as a Newtonian fluid (that is to say, the stress exponent n is equal to 1). Recent laboratory experiments [*Goldsby and Kohlstedt*, 1997], performed for small grain sizes and strain rates >10^{-8} s^{-1}, suggested that creep is controlled by grain boundary sliding, with n ~ 2. The flow is not Newtonian, but the stress dependence is weaker than for dislocation creep (n = 3). A more important source of uncertainties is the lack of constraints on the parameters of the viscosity law (equation (11)). The results of *Goldsby and Kohlstedt* [1997], in agreement with previous studies [e.g., *Durham et al.*, 1997], suggested that a possible value of the activation energy yields between 49 and 62 kJ/mol. For such values of E, heat transfer by convection is efficient enough to complete the crystallization of the initial ocean. However, one cannot exclude higher values. For instance, if E = 90 kJ/mol and $\mu_0 = 5\times10^{13}$ Pa s, the mean heat flux is only 7.8 mW/m^2, and the characteristic time of cooling is ~8.8 Gyr. Similarly, the vigor and the efficiency of convection decrease significantly as the reference viscosity increases. For values of μ_0 higher than or equal to 10^{14} Pa s, and unless E is small (~40 kJ/mol), the convective heat flux is smaller than 16 mW/m^2 (Table 5), and the characteristic time of cooling is higher than 4.3 Gyr. Therefore, if the reference viscosity of ice I is higher than 10^{14} Pa s, a residual subsurface ocean probably exists in icy satellites. On the other hand, simple estimations based on laboratory [*Goldsby and Kohlstedt*, 1997] and field [*Gerrard et al.*, 1952] experiments suggest smaller values for μ_0. According to these studies, the reference viscosity μ_0 likely yields values around 5×10^{13} Pa s.

The presence of volatiles in the initial ocean weakens the convection in the ice I layer. Moreover, if the ice layer is too thick, the convection stops. In this study we have conducted calculations for a mixture of water and ammonia. However, *Kargel* [1998] pointed out that ammonia is unstable with respect to many other possible components of the primordial ocean, such as H_2S, CO_2, Na_2SO_4, and $MgSO_4$. Therefore ammonia was probably not present in the primordial ocean. However, we believe that the presence of any other volatile would induce some consequences comparable to those induced by the presence of ammonia. Assuming E = 60 kJ/mol and $\mu_0 = 5\times10^{13}$ Pa s, the energy E_c is completely released in <4.55 Gyr only for values of the initial ammonia ratio (x_{NH3}) smaller than 3%. If one considers smaller values of the activation energy (e.g., E = 40 kJ/mol) or of the reference viscosity (e.g., $\mu_0 = 10^{13}$ Pa s), the convective heat flux is higher than 15 mW/m^2 for x_{NH3} = 10%, but not for x_{NH3} = 15% (Table 6). Therefore the presence of volatiles in the primordial ocean could have stopped the crystallization of the ocean, and a residual ocean may exist below the outer ice I layer. Recently, *Khurana et al.* [1998] suggested that the magnetic perturbations recorded near Callisto could be explained by the presence of a subsurface ocean. Moreover, if volatiles are present, the thickness of the lithosphere increases strongly. In other words, the lithosphere is more resistant to tectonic stress, and convection would probably not induce tectonic features on the surface. This result could explain why there are nearly no tectonic features at the surface of Callisto, whereas Ganymede, which is comparable in size, has been tectonically very active. Indeed, a possible explanation is that the initial ocean of Callisto was significantly richer in ammonia than that of Ganymede. This hypothesis implies that the protoplanetary nebula was not homogeneous during the accretion of the icy satellites. A possible explanation for such heterogeneities could be a decrease of the temperature as the distance from Jupiter increases, allowing

Table 7. Properties of Long-Lived Radioisotopes[a]

Isotope	h, 10^{-5} W/kg	C, ppm	H, 10^{-12} W/kg		λ, Gyr^{-1}
			t = 4.55 Gyr	t = 0	
^{235}U	56.9	0.1	0.057	5.04	0.985
^{238}U	9.37	12.9	1.21	2.45	0.155
^{232}Th	2.69	40	1.08	1.35	0.0495
^{40}K	2.79	100	2.79	34.9	0.555

[a] *Turcotte and Schubert* [1982, pp. 140-141]. h is the radiated power per kilo of isotope, C is the chondritic concentration at t = 4.55 Gyr, and λ the decay constant of the radioisotope. The radiated power per kilo of rock is therefore $H = Che^{\lambda t}$ at t = 0, and $H = Ch$ at t = 4.55 Gyr.

volatiles to condense mostly at the periphery of the nebula. However, such a model has not been proposed for the moment.

The estimated heat flux at the top of the core is produced by the decay of radioactive elements present in silicates. It is important to note that this heat flux does not depend on the satellite mean density and radius. The model of *Kirk and Stevenson* [1987] includes the heat losses during the transfer through the silicate shell. On the other hand, it does not account for possible additional heat sources.

A first additional source of energy could be provided by the cooling of an iron core. Indeed, the recent measurement performed by Galileo suggested that Ganymede has an iron core [*Anderson et al.*, 1996]. However, a simple calculation shows that it can be neglected to the first order. If one assumes that the pressure at the center of the iron core yields between 3 and 7 GPa, the melt temperature of the iron core is about 1830-1870 K, and the latent heat (L_c) lies between 270 and 280 kJ/kg [*Poirier*, 1991, pp. 101-108]. Moreover, in this range of pressure the density of iron is about ρ_c = 7-8 g/cm^3. Therefore, if the core radius is r_c = 1000 km, the energy released would be approximately $E_{Fe} = 8\times10^{27}$-10^{28} J. Taking the maximal value, $E_{Fe} = 10^{28}$ J, and assuming that the cooling of the core is completed in 1 Gyr, the additional heat flux at the bottom of a 150 km thick layer of ice I would be only 0.9 mW/m^2. This increment is small and in the case of the generic satellite can be fully transported by the convective ice I layer. Similarly, one must consider the energy released by the crystallization of ices. For instance, let us consider a generic satellite (radius R = 2500 km; radius of the silicate mantle r_s = 1900 km). The crystallization of a 150 km thick layer of ice I (latent heat L_I = 284 kJ/kg and density ρ_I = 917 kg/m^3) provides approximately E_I ~ 3×10^{27} J. The crystallization of a 300 km thick layer of high-pressure ices (L_{HP} = 294 kJ/kg and ρ_{HP} = 1310 kg/m^3) releases E_{HP} ~ 6×10^{27} J. Therefore the crystallization of a water shell and of an iron core provides an average heat flux around 2 mW/m^2, if averaged along 1 Gyr. Finally, it must be pointed out that the efficiency of heat transfer across the mantle of high-pressure ices is supposed to be more efficient than that through the outer ice I layer. If this heat transfer is not efficient enough, the energy generated by the cooling of the core cannot be transferred in the ocean, and the HP ices shell would act as an additional insulator.

Another additional source of energy, which has been neglected in this study, is the energy released by tidal dissipation. Tides result from variations of the gravitational potential along an eccentric orbit. The amount of energy dissipated per second is deduced from the Love numbers of the satellite, which describe the normal modes of deformation. Given a model for the internal of a satellite, it is possible to compute the Love numbers [e.g., *Castillo et al.*, 2000]. The effect of tidal dissipation can be estimated by considering an additional heat flux at the base of the outer ice layer. For Ganymede, values of 2-5 mW/m^2 are found. This heat flux is small, and therefore convection may be able to transfer tidal heat toward the surface. However, a high value of Ganymede's eccentricity in the past may have induced larger tidal heat flux, as suggested by *Malhotra* [1991]. On the other hand, Callisto would have never experienced a highly elliptical orbit. This may explain why resurfacing occurred on Ganymede but not on Callisto [*Showman and Malhotra*, 1999]. In the case of Europa the tidal heat production may be large [*Showman and Malhotra*, 1999], and convection may be too inefficient to transfer this additional heat toward the surface.

Finally, the scaling laws used in the present study do not account for internal heating. However, one expects that the efficiency of heat transfer decreases as the internal heating increases. For instance, in an isoviscous fluid heated both from below and from within, hot plumes are less vigorous [*Parmentier et al.*, 1994; *Sotin and Labrosse*, 1999]. Similar observations can be made using our numerical model of convection. For a given Rayleigh number, the temperature of the well-mixed interior increases and the bottom heat flux decreases as the rate of internal heating increases. In other words, convection is less efficient at releasing the energy supplied at the bottom of the convective fluid.

5. Conclusion

Convection in the outer layer of a large icy satellite controls the cooling history of the satellite. The present internal structure of the satellite depends strongly on the ability of the outer layer to transfer heat. The efficiency of convection depends strongly on rheological and compositional parameters. Some uncertainties remain on the parameters of the viscosity law as well as on the flow regime. With currently accepted values of E and μ_0 close to 60 kJ/mol and 5×10^{13} Pa s, respectively, convection is efficient enough to complete the crystallization of the initial ocean in about ~4 Gyr. This result suggests that the freezing of an internal liquid shell is not a rapid geological event (<100 Myr) but may have occurred very recently in the history of large icy satellites. Moreover, the presence of volatiles inhibits convection and favors the existence of a residual ocean. We propose that the composition of the primordial ocean significantly influences the tectonic activity and the present-day upper structure of the large icy satellites. A residual subsurface ocean may have subsisted, as it is expected for Callisto. Internal heating induced by tidal dissipation probably plays an important role as well and may constitute another way to maintain a subsurface ocean. The goal of the present paper was to describe the different parameters that influence the cooling history of large icy satellites, using scaling laws appropriate to describe convective heat transfer through strongly temperature-dependent viscosity fluids. Forthcoming papers will use these scaling laws to model the evolution of icy satellites. It is worth emphasizing that laboratory experiments are required to get better knowledge of ice (H_2O+volatiles) phase diagrams and creep behavior.

Acknowledgements. We would like to thank D. Stevenson and S. Solomatov for useful reviews, which helped to improve a first version of this paper. This work was supported by a grant of CNRS-INSU, Programme National de Planétologie.

References

Anderson, J.D., E.L. Lau, W.L. Sjorgren, G. Schubert, and W.B. Moore, Gravitational constraints on the internal structure of Ganymede, *Nature*, *384*, 541-543, 1996.

Anderson, J.D., G. Schubert, R.A. Jacobson, E.L. Lau, W.B. Moore, and W.L. Sjogren, Distribution of rock, metals and ices in Callisto, *Science*, *280*, 1573-1576, 1998a.

Anderson, J.D., G. Schubert, R.A. Jacobson, E.L. Lau, W.B. Moore and W.L. Sjogren, Europa's differentiated internal structure: inferences from four Galileo encounters, *Science*, *281*, 2019-2022, 1998b.

Bercovici, D., G. Schubert, and R.T. Reynolds, Phase transitions and convection in icy satellites, *Geophys. Res. Lett.*, *13*, 448-451, 1986.

Bergholz, R.F., M.M. Chen, and F.B. Cheung, Generalization of heat-transfer results for turbulent free convection adjacent to horizontal surfaces, *Int. J. Heat Mass Transfer*, *22*, 763-769, 1979.

Boone, S., and M.F. Nicol, Ammonia-water mixtures at high pressures: melting curves of ammonia-dihydrate and ammonia monohydrate and a revised high-pressure phase diagram for the water-rich region, *Proc. Lunar Planet. Sci. Conf. 21st*, 603-612, 1991.

Carr, M.H., M.J.S. Belton, C.R. Chapman, M.E. Davies, and P. Geissler,

Evidence for a subsurface ocean on Europa, *Nature, 391*, 363-365, 1998.

Cassen, P.M., S.J. Peale, and R.T. Reynolds, Structure and thermal evolution of the galilean satellites, in *The Satellites of Jupiter*, edited by D. Morrison, pp. 93-128, Univ. of Ariz. Press, Tucson, 1981.

Castillo, J., A. Mocquet, and C. Sotin, Détecter la présence d'un océan dans Europe à partir de mesures altimétriques et gravimétriques, *C.R. Acad. Sci. Ser. 2, 330*, 659-666, 2000.

Chizhov, V.E., Thermodynamic properties and equation of state of high-pressure ice phases, *Prikl. Mekh. Tekh. Fiz.*, Engl. Transl., *2*, 113-123, 1993.

Choblet, G., and Sotin C., 3D thermal convection with variable viscosity: Can transient cooling be described by a quasi-static scaling law?, *Phys. Earth Planet. Inter., 119*, 321-336, 2000.

Christensen, U.R., Heat transport by variable viscosity convection and implications for the Earth's thermal evolution, *Phys. Earth Planet. Inter., 35*, 264-282, 1984.

Consolmagno, G.J., and J.S. Lewis, Structural and thermal models of icy galilean satellites, in *Jupiter*, edited by T.A. Gehrels, pp. 1035-1051, Univ. of Ariz. Press, Tucson, 1976.

Davaille, A., and C. Jaupart, Transient high-Rayleigh-number thermal convection with large viscosity variations, *J. Fluid Mech., 253*, 141-166, 1993.

Deschamps, F., and C. Sotin, Inversion of 2D numerical convection experiments for a strongly temperature-dependent viscosity fluid heated from below, *Geophys. J. Int., 143*, 204-218, 2000.

Dumoulin, C., M.-P. Doin, and L. Fleitout, Heat transport in stagnant lid convection with temperature- and pressure-dependent Newtonian or non-Newtonian rheology, *J. Geophys. Res., 104*, 12,759-12,777, 1999.

Durham, W.B., S.H. Kirby, and L.A. Stern, Creep of water ices at planetary conditions: a compilation, *J. Geophys. Res., 102*, 16,293-16,302, 1997.

Forni, O., C. Frederico, A. Coradini, and G. Magni, Origin and evolution of comets, icy planets and satellites, in *Solar System Ices*, edited by B. Schmitt et al., pp. 367-394, Kluwer Acad., Norwell, Mass., 1998.

Friedson, A.J., and D.J. Stevenson, Viscosity of rock-ice mixtures and application to the evolution of icy satellites, *Icarus, 56*, 1-14, 1983.

Gerrard, J.A.F., M.F. Perutz, and A. Roch, 1952, Measurement of the velocity distribution along a vertical line through a glacier, *Proc. R. Soc. London, Ser. A, 207*, 554-572, 1952.

Goldsby, D.L., and D.L. Kohlstedt, Grain boundary sliding in fine-grained Ice-I, *Scr. Mater., 37*, 1399-1405, 1997.

Goodman, D.J., H.J. Frost, and M.F. Ashby, The plasticity of polycristalline ice, *Philos. Mag. A, 43*, 665-695, 1981.

Grasset, O., and E.M. Parmentier, Thermal convection in a volumetrically heated, infinite Prandtl number fluid with strongly temperature-dependent viscosity: Implications for planetrary thermal evolution, *J. Geophys. Res., 103*, 18,171-18,181, 1998.

Grasset, O., and C. Sotin, The cooling rate of a liquid shell in Titan's interior, *Icarus, 123*, 101-112, 1996.

Grasset, O., S. Beauchesne, and C. Sotin, Investigation of the NH_3-H_2O phase diagram in the range 100 MPa-1.5 GPa using in-situ Raman spectroscopy: Application to Titan's dynamics, *C. R. Acad. Sci. Ser. 2, 320*, 249-256, 1995.

Grasset, O., C. Sotin, and F. Deschamps, On the internal structure and dynamics of Titan, *Planet. Space Sci., 48*, 617-636, 2000.

Hobbs, P.V., Ice Physics, 837 pp., Oxford Univ. Press, New York, 1974.

Hogenboom, D.L., J.S. Kargel, G. Consolmagno, T.C. Holden, L. Lee, and M. Buyyounouski, The amonia-water system and the chemical differentiation of icy satellites, *Icarus, 128*, 171-180, 1997.

Johnson, M.L., and M. Nicol, The ammonia-water phase diagram and its implications for icy satellites, *J. Geophys. Res., 92*, 6339-6349, 1987.

Kargel, J.S., Composition of Europa's ocean and crust, in *Lunar Planet. Sci.* [CD-ROM], *XXIX*, abstract 1418, 1998.

Khurana, K.K., M.G. Kivelson, D.J. Stevenson, G. Schubert, C.T. Russell, R.J. Walker, and C. Polanskey, Induced magnetic fields as evidence for subsurface oceans in Europa and Callisto, *Nature, 395*, 777-780, 1998.

Kirk, R.L., and D.J. Stevenson, Thermal evolution of a differenciated Ganymede and implications for surface features, *Icarus, 69*, 91-134, 1987.

Kivelson, M.G., K.K. Khurana, C.T. Russell, M. Volwerk, R.J. Walker, and C. Zimmer, Galileo magnetometer measurements: A stronger case for a subsurface ocean at Europa, *Science, 289*, 1340-1343, 2000.

Lewis, J.S., Satellites of the outer planets: Their physical and chemical nature, *Icarus, 15*, 175-185, 1971.

Lunine, J.I., and D.J. Stevenson, Formation of the galilean satellites in a gaseous nebula, *Icarus, 52*, 14-39, 1982.

Malhotra, R., Tidal origin of the Laplace resonance and the resurfacing of Ganymede, *Icarus, 94*, 399-412, 1991.

McKinnon, W.B., Thermodynamic properties of high pressure ices: Implications for the dynamics and internal structure of large icy satellites, in *Solar System Ices*, edited by B. Schmitt et al., pp. 525-550, Kluwer acad., Norwell, Mass., 1998.

Moresi, L.-N., and V.S. Solomatov, Numerical investigation of 2-D convection with extremely large viscosity variations, *Phys. Fluids, 7*, 2154-2162, 1995.

Morris, S., and D. Canright, A boundary-layer analysis of Bénard convection in a fluid of strongly temperature-dependent viscosity, *Phys. Earth Plant. Inter., 36*, 355-373, 1984.

Mueller, S., and W.B. McKinnon, Three-layered models of Ganymede and Callisto: Composition, structures and aspects of evolution, *Icarus, 76*, 437-464, 1988.

Nataf, H.-C., and F.M. Richter, Convection experiments with highly temperature-dependent viscosity and the thermal evolution of the planets, *Phys. Earth Planet. Inter., 32*, 320-329, 1982.

Ogawa, M., G. Schubert, and A. Zebib, Numerical simulations of three-dimensional thermal convection in a fluid with strongly temperature-dependent viscosity, *J. Fluid Mech., 233*, 299-328, 1991.

Parmentier, E.M., C. Sotin, and B.J. Jarvis, Turbulent 3-D thermal convection in an infinite Prandtl number, vollumetrically heated fluid: Implications for mantle dynamics, *Geophys. J. Int., 116*, 241-251, 1994.

Poirier, J.P., Introduction to the Physics of the Earth Interior, 264 pp., Cambridge Univ. Press, New York, 1991.

Prinn, R.G., and B. Fegley, Solar nebula chemistry: Origin of planetary, satellite, and cometary volatiles, in *Origin and Evolution of Planetary and Satellite Atmospheres* edited by S.K. Atreya, J.B. Pollack, and M.S. Matthews, pp. 78-136, Univ. of Ariz. Press, Tucson, 1989.

Reese, C.C., V.S. Solomatov, and L.-N. Moresi, Non-Newtonian stagnant lid convection and magmatic resurfacing on Venus, *Icarus, 139*, 67-80, 1999.

Reynolds, R.T., and P.M. Cassen, On the internal structure of the major satellites of the major planets, *Geophys. Res. Lett., 6*, 121-124, 1979.

Schubert, G., P. Cassen, and R.E. Young, Subsolidus convective cooling of terrestrial planets, *Icarus, 38*, 192-211, 1979.

Schubert, G., D. J. Stevenson, and K. Ellsworth, Internal structures of the galilean satellites, *Icarus, 47*, 46-59, 1981.

Showman, A.P., and R. Malhotra, The Galilean satellites, *Science, 286*, 77-84, 1999.

Sotin, C., and E.M. Parmentier, On the stability of a fluid layer containing a univariant phase transition: Application to planetary interiors, *Phys. Earth Planet. Inter., 55*, 10-25, 1989.

Sotin, C., O. Grasset, and S. Beauchesne, Thermodynamic properties of high pressure ices: implications for the dynamics and internal structure of large icy satellites, in *Solar System Ices*, edited by B. Schmitt et al., pp. 76-96, Kluwer Acad., Norwell, Mass., 1998.

Sotin, C., and S. Labrosse, Thermal convection in an isoviscous, infinite Prandtl number fluid heated from within and from below: Applications to heat transfer through planetary mantles, *Phys. Earth Planet. Inter., 122*, 171-190, 1999.

Turcotte, D.L., and G. Schubert, Geodynamics: Application of Continuum Physics to Geological Problems, 450 pp., John Wiley, New York, 1982.

Weertman, J., Dislocation climb theory of steady-state creep, *AMS Trans. Q., 61*, 681-694, 1968.

Weertman, J., Creep deformation of ice, *Annu. Rev. Earth Planet. Sci., 11*, 215-240, 1983.

White, D.B., The planforms and onset of convection with a temperature-dependent viscosity, *J. Fluid Mech., 191*, 247-286, 1988.

Zimmer, C., K.K. Khurana, and M.G. Kivelson, Subsurface oceans on Europa and Callisto: Constraints from Galileo magnetometer observations, *Icarus, 147*, 329-347, 2000.

F. Deschamps, Faculty of Earth Sciences, Utrecht University, PO Box 80021, 3508 TA Utrecht, The Netherlands. (deschamp@geo.uu.nl)

C. Sotin, Laboratoire de Planétologie et Géodynamique, UMR-CNRS 6112, Université de Nantes, BP 92208, 44322 Nantes, France. (sotin@chimie.univ-nantes.fr)

(Received March 14, 2000; revised October 20, 2000;
accepted October 29, 2000.)